research articles Journal of proteome research

Proteomic Analysis of Human Nail Plate

Robert H. Rice,*,† Yajuan Xia,‖ Rudy J. Alvarado,§ and Brett S. Phinney§

Department of Environmental Toxicology, University of California, Davis, California 95616, United States, Inner Mongolia Center for Endemic Disease Control and Research, Huhhot, Inner Mongolia, China, and Genome Center Proteomic Core Facility, University of California, Davis, California 95616, United States

Received September 14, 2010

Shotgun proteomic analysis of the human nail plate identified 144 proteins in samples from Causcasian volunteers. The 30 identified proteins solubilized by detergent and reducing agent, 90% of the total nail plate mass, were primarily keratins and keratin associated proteins. Keratins comprised a majority of the detergent-insoluble fraction as well, but numerous cytoplasmic, membrane, and junctional proteins and histones were also identified, indicating broad use by transglutaminases of available proteins as substrates for cross-linking. Two novel membrane proteins were identified, also found in the hair shaft, for which mRNAs were detected only at very low levels by real-time polymerase chain reaction in other tissues. Parallel analyses of nail samples from volunteers from Inner Mongolia, China gave essentially the same protein profiles. Comparison of the profiles of nail plate and hair shaft from the latter volunteers revealed extensive overlap of protein constituents. Analyses of samples from an arsenic-exposed population revealed few proteins whose levels were altered substantially but raised the possibility of detecting sensitive individuals in this way.

Keywords: Junctional proteins • Keratins • LRRC15 • Transglutaminase • VSIG8

Introduction

Abnormalities in the nail can reflect environmental exposures, systemic disease, or genetic disease. An indication of the prevalence of such effects, brittle nail syndrome, occurs in ≈20% of the population.[1] A variety of systemic disorders have manifestations in nail appearance and function, and numerous drugs and toxic ingestants affect nail biosynthesis.[2,3] Some treatments or conditions, including rare genodermatoses, produce leukonychia ("white nails"), often attributed to perturbation of the differentiation of cells exiting the matrix.[4] For example, acute arsenic poisoning can produce transverse white striations (Mees' lines) that reflect the period of exposure.[5] A dozen genodermatoses are recognized with prominent nail anomalies and twice as many with combined nail and hair anomalies.[6]

The human nail unit displays an intricate differentiation program to produce the nail plate. Resemblance of the program to that in both hair and epidermis became evident as methods developed to distinguish among the many keratin proteins expressed.[7,8] Refinements led to improved localization in the nail matrix of cells expressing hard (hair) or soft (epidermal) keratins or both, and to finding distinctive keratin expression patterns there compared to those in the proximal nail fold and nail bed.[9,10] The fine structure of the patterns indicates that the nail plate is generated primarily by the ventral matrix with a contribution by the apical matrix to the dorsal portion.[11] The nail plate is held firmly in place by interdigitations on the underside with the nail bed, which is histologically distinct from the matrix.[12]

Although differing in terminal differentiation from epidermis in some details, such as lack of a granular layer or caspase-14 expression,[13] the matrix produces a nail plate comprised largely of keratins, accounting for its mechanical resistance to environmental insult. Contributing to the mechanical strength are interdigitations between neighboring cornified cells and disulfide cross-linking among the constituent proteins. Cells of the nail plate also display considerable isopeptide cross-linking, visible after extensive extraction with detergent and reducing agent[14] and whose deficiency is demonstrable in TGM1-negative lamellar ichthyosis.[15] Present experiments were designed to identify prominent constituents of the cross-linked component, to compare them to those found in the hair shaft, and to find whether the composition was altered by chronic arsenic exposure. A useful indicator of arsenic exposure from well water,[16] the nail plate provides a convenient noninvasive sampling of proteins for proteomic analysis.

Materials and Methods

Nail and Hair Samples. One set of four fingernail clippings was analyzed from Caucasian volunteers at the University of California, Davis. A second set of fingernail and the hair samples (four each) were analyzed from volunteers in Inner Mongolia.[16] In the latter group, those with low exposure (two males, two females) drank well water containing 0.1 ppb arsenic, and those with high exposure (two males, two females)

* To whom correspondence should be addressed. Dr. Robert H. Rice, Department of Environmental Toxicology, University of California, One Shields Avenue, Davis, CA 95616-8588. Tel 530-752-5176. Fax 530-752-3394. E-mail: rhrice@ucdavis.edu.

† Department of Environmental Toxicology, University of California.

‖ Inner Mongolia Center for Endemic Disease Control and Research.

§ Genome Center Proteomic Core Facility, University of California.

10.1021/pr1009349

Published on Web 10/12/2010

drank well water containing 456−536 ppb arsenic. The nail samples from Mongolia were cleaned by sonication in HPLC-grade water, followed by an acetone wash to remove water and organic contamination from the nail surface.[16] All samples were obtained from nonsmokers with written informed consent according to the recommendations of the Declaration of Helsinki (http://www.wma.net/en/30publications/10policies/b3/index.html).

Proteomic Sample Preparation. As previously described[17] with minor modifications, samples of nail plate or hair shaft (20 mg) were rinsed briefly in 2% sodium dodecyl sulfate to remove loosely adhering contaminants, incubated overnight at 70 °C in 5 mL of 2% sodium dodecyl sulfate/0.1 M sodium phosphate (pH 7.8)/20 mM dithioerythritol, and pulverized by stirring for several hours with a small magnetic stirring bar. Insoluble material was recovered by centrifugation and extracted 4 more times, with the protein content of the extract being monitored to ensure complete extraction. (Virtually no protein was recovered in the final extraction supernatant.) The fraction of insoluble protein was 11 + 3% from nail samples. The soluble and insoluble fractions were alkylated with iodoacetamide and digested for 3 days at room temperature with reductively methylated trypsin[18] in fresh 0.1 M ammonium bicarbonate containing 10% acetonitrile. As for hair previously,[17] >90% of the nail sample protein was solubilized by the trypsin digestion. Peptides were dried down in a vacuum concentrator after digestion, then resolubilized in 2% acetonitrile/0.1% trifluoroacetic acid for LC−MS/MS analysis.

Mass Spectrometry. Digested peptides were analyzed using LC−MS/MS on an LTQ with Michrom Paradigm LC and CTC Pal autosampler. Peptides were directly loaded onto an Agilent ZORBAX 300SB C_{18} reverse-phase trap cartridge which, after loading, was switched in-line with a Michrom Magic C18 AQ 200 μm ×150 mm C18 column connected to a Thermo-Finnigan LTQ iontrap mass spectrometer through a Michrom Advance Plug and Play nanospray source. The nano-LC column (Michrom 3 μm, 200 Å MAGIC C18AQ, 200 μm × 150 mm) was used with a binary solvent gradient; buffer A was composed of 0.1% formic acid and buffer B composed of 100% acetonitrile. The 120 min gradient consisted of the steps 2−35% buffer B in

Table 1. Proteins Identified in the SDS/DTE Solubilized and Insoluble (Cross-Linked) Fractions of Human Nail Plate Listed in Decreasing Order of Estimated Abundance (emPAI[a])

		cross-linked				solubilized	
protein[b]	MW (kDa)	emPAI	peptides[c]	protein[b]	MW (kDa)	emPAI	peptides[c]
KRT86	53	10.6	172	KRT86	53	29.2	327
KRT81	55	8.6	14	KRT33B	46	24.5	224
KRT33B	46	6.7	109	KRT81	55	17.3	26
KRT34	45	6.2	61	KRT34	45	9.7	78
KRT31	47	5.3	42	KRT85	56	9.0	165
KRTAP13-2	19	4.2	46	KRT83	54	5.4	33
KRTAP13-1	21	4.2	38	KRT16	51	1.0	77
KRT85	56	3.0	50	KRT14	52	0.8	105
LRRC15	64	2.8	136	KRT36	52	0.7	71
KRTAP13-4	18	2.8	53	KRT84	65	0.6	101
KRTAP11-1	17	2.5	23	KRTAP13-4	18	0.6	22
HIST1H4D	11	2.4	27	KRT6A	60	0.4	106
PRDX6	25	2.3	45	KRT17	48	0.4	49
KRT83	54	2.2	10	KRT5	62	0.2	43
SFN	28	1.8	44	KRTAP13-2	19	0.2	26
LGALS7	15	1.8	27	KRTAP13-1	21	0.2	21
JUP	82	1.7	112	KRTAP2-4	13	0.1	23
FABP4	15	1.7	34	KRT1	66	0.06	26
TAGLN2	22	1.7	29	KRTAP11-1	17	0.06	13
SELENBP1	57	1.6	85	LRRC15	64	0.05	40
HSPB1	23	1.4	40	KRT39	56	0.05	30
HIST1H2AH	14	1.3	32	KRT32	50	0.04	23
KRT84	65	1.1	63	DSP	332	0.02	64
VSIG8	44	1.1	62				
CALML3	17	1.1	20				
FABP5	15	1.1	20				
DSP	332	1.0	348				
LAP3	56	1.0	46				
PKP1	80	0.9	88				
KRT14	52	0.8	46				
GAPDH	36	0.8	34				
KRTAP2-4	13	0.7	29				
CRYAB	20	0.7	19				
ACTB	42	0.6	51				
EEF1A1	50	0.6	37				
ANXA1	39	0.6	30				
CALML5	16	0.6	20				
YWHAZ	28	0.6	19				

[a] Exponentially modified protein abundance index. The 38 proteins listed for the insoluble fraction (total 82) account for 90% of the total emPAI in that fraction. See Table S2 for calculations. [b] emPAI values were calculated only for the proteins detected in all four nail plate samples. [c] Each value is the sum of unique peptides for the four samples analyzed.

85 min, 35−80% buffer B in 23 min, hold for 1 min, 80−2% buffer B in 1 min, then hold for 10 min, at a flow rate of 2 μL/min for the maximum separation of tryptic peptides. MS and MS/MS spectra were acquired using a top 10 method, where the top 10 ions in the MS scan were subjected to automated low energy CID. An MS survey scan was obtained for the m/z range 375−1400, and MS/MS spectra were acquired using the three most intense ions from the survey scan. An isolation mass window of 2 Da was used for the precursor ion selection, and a normalized collision energy of 35% was used for the fragmentation. A 2 min duration was used for the dynamic exclusion.

Protein Identification. Tandem mass spectra were extracted with Xcalibur version 2.0.7. All MS/MS samples were analyzed using X! Tandem (www.thegpm.org; version TORNADO (2008.02.01.2)). X! Tandem was set up to search the IPI human database (version 3.59, 79 736 entries) assuming the digestion enzyme trypsin. X! Tandem was searched with a fragment ion mass tolerance of 0.40 Da and a parent ion tolerance of 1.8 Da. Iodoacetamide derivative of cysteine was specified in X! Tandem as a fixed modification. Oxidation of methionine and acetylation of the N-terminus were specified in X! Tandem as variable modifications. Scaffold (version Scaffold_2_01_01, Proteome Software, Inc., Portland, OR) was used to validate MS/MS based peptide and protein identifications. Peptide identifications were accepted if they could be established at greater than 80% probability as specified by the Peptide Prophet algorithm.[19] Protein identifications were accepted if they could be established at greater than 99.0% probability and contained at least 2 identified peptides. Protein probabilities were assigned by the Protein Prophet algorithm.[20] Proteins that contained similar peptides and could not be distinguished by MS/MS analysis alone were grouped for parsimony. Numbers of unique peptides were tabulated as a basis for selecting prominent proteins for further analysis.

Estimates of Relative Abundance. Using samples generated from the four Caucasian donors, emPAI values were obtained from Mascot searches of the IPI human database (version 3.59, 79 736 entries) assuming semitryptic cleavages. As previously performed,[21,22] parameters for searching included a fragment ion mass tolerance of 0.6 Da, a parent ion tolerance of 2.5 Da, carbamidomethylation of cysteine as a fixed modification, oxidation of methionine as a variable modification and a cutoff score of 35. emPAI values were tabulated for the four nail samples in a given category (solubilized, insoluble). Estimates of relative molar amount were calculated by normalizing to the total emPAI values for a given category.[23]

Real-Time Polymerase Chain Reaction. Commercial preparations of normalized cDNA from pooled human tissues (Human Multiple Tissue cDNA Panels I and II from Clontech, Mountain View, CA) were interrogated using TaqMan gene expression assay probes (AppliedBiosystems, Foster City, CA) in duplicate in an ABI 7500 Fast Sequence Detection System. For comparison, cDNA was prepared from RNA from foreskin epidermis obtained from skin by heat treatment[24] and confluent cultures[25] using a High Capacity cDNA Archive Kit (Applied Biosystems) after extraction with Trizol (Invitrogen, Carlsbad, CA) and DNase treatment (DNA-free kit from Ambion/Applied Biosystems); cDNA samples from 50 ng of total RNA were employed per measurement. Data presented are Ct values (cycles required to reach threshold fluorescence), inversely proportional to antilog (base 2) of mRNA amount.

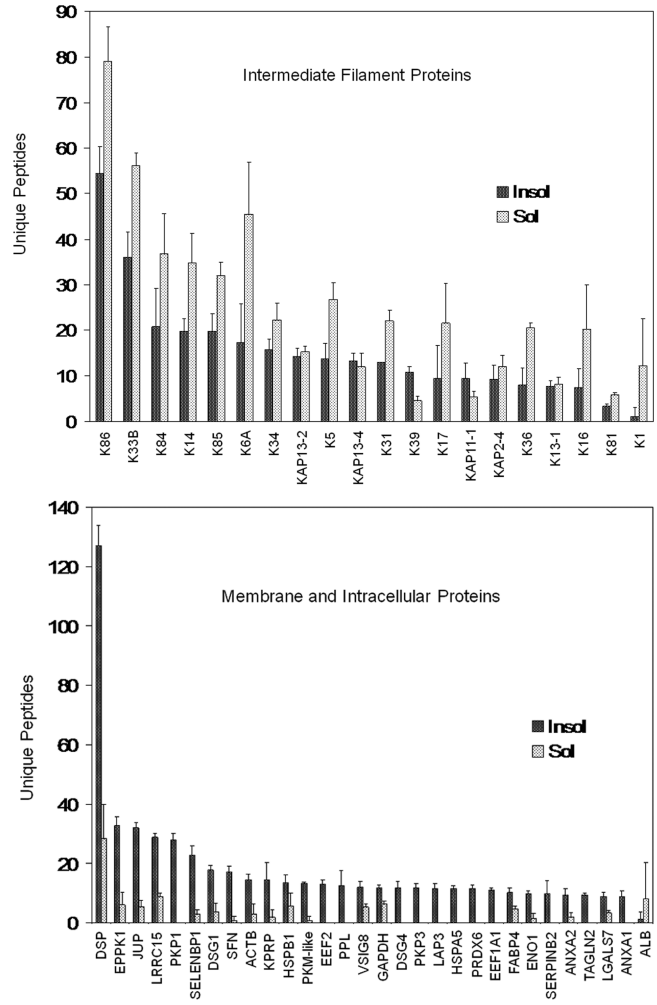

Figure 1. Comparison of yields obtained from the solubilized versus insoluble fractions from nail plate. The 50 proteins with the highest number of unique peptides are grouped as cytoskeletal (keratins and keratin associated proteins) and membrane and intracellular proteins (the remainder). Illustrated are means and standard deviations of 4 samples.

Multiple Reaction Monitoring. Potential proteotypic peptides from the Global Proteome Machine Database (http://www.gpmdb.org/) for a given protein were BLASTed to verify uniqueness and examined for prevalence in the Scaffold files of samples analyzed to date. Characteristic transitions in the fragmentation patterns of the several candidate peptides were then examined using a Thermo TSQ Vantage triple quadrupole mass spectrometer with a Michrom Paradigm LC and CTC Pal Autosampler. Peptides were directly loaded onto an Agilent ZORBAX 300SB C18 reverse-phase trap cartridge which, after loading, was switched in-line with a Michrom Magic C18 AQ 200 μm $\times$150 mm C18 column connected to a Thermo TSQ Vantage triple quadrupole mass spectrometer through a Michrom Advance Plug and Play nanospray source. The nano-LC column (Michrom 3 μm, 200 Å MAGIC C18AQ, 200 μm $\times$ 150 mm) was used with a binary solvent gradient; buffer A was composed of 0.1% formic acid and buffer B composed of 100% acetonitrile. The 45 min gradient consisted of the steps 2−35% buffer B in 30 min, 35−80% buffer B in 1 min, hold for 5 min, 80−2% buffer B in 1 min, then hold for 8 min, at a flow rate of 2 μL/min for the maximum separation of tryptic peptides. Ionization and acquisition parameters were the following, Q2

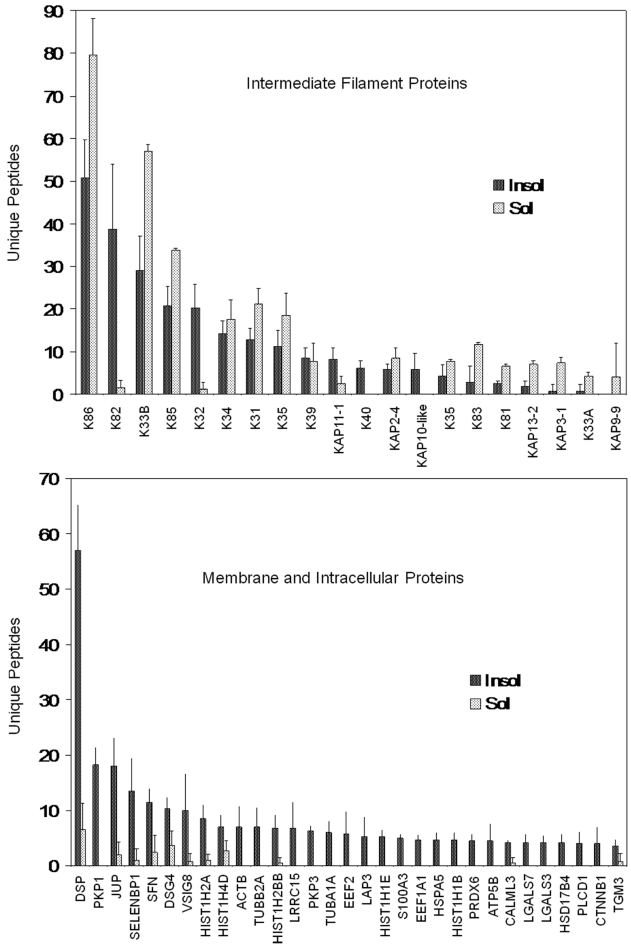

Figure 2. Comparison of yields obtained from the solubilized versus insoluble fractions from hair shaft. The 50 proteins with the highest number of unique peptides are grouped as cytoskeletal (keratins and keratin associated proteins) and membrane and intracellular proteins (the remainder). Illustrated are means and standard deviations of 4 samples.

collision gas pressure = 1.2 mTorr of argon, Q1 and Q3 selectivity = 0.7 Da (FQHM), spray voltage = 1900 V, capillary temp = 180 °C. S-Lens and collision energy was optimized for each individual peptide using the isotope labeled peptide analogues detailed below. The best candidate peptides were used for reanalysis of the samples, each spiked with 500 fmol of isotopically labeled peptide analogues (Heavy Peptide AQUA, Thermo Scientific Custom Peptides). The proteotypic peptides employed were SPNQNVQQAAAGALR (PKP1) and IQVVDVR (DSG4). Yields of 3−4 transitions normalized to those of the isotopically peptides were monitored.

Proteomics Data Set. The data associated with this manuscript may be downloaded from ProteomeCommons.org Tranche using the following hash:

zQPrT/Z8UF3rDGwhHKMr6FEZNFvEwDr+94GublvAunowL+M3as/lrQF77dcQfWRyH35ANN4wCxFSoDK6HnvGto+QbG8AAAAAAAAf9A==.

The hash may be used to prove what files were published as part of this manuscript's data set and to check that the data have not changed since publication.

Results

To identify prominent protein constituents in nail plate and to compare them to those in hair shaft, shotgun proteomic

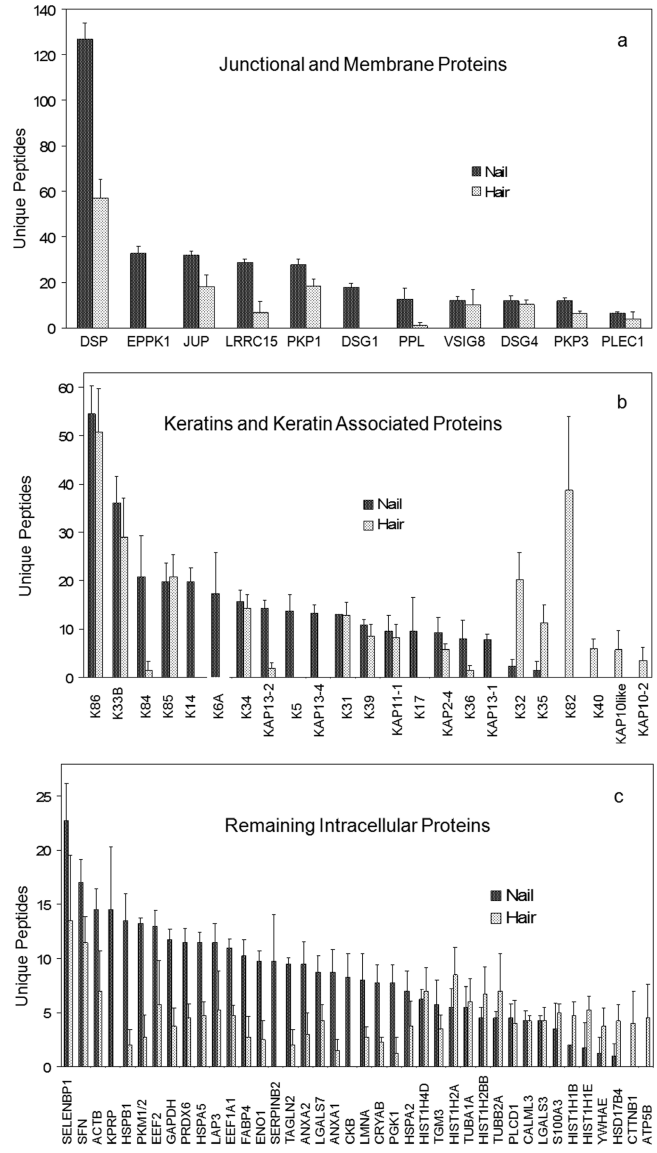

Figure 3. Overlapping protein expression in nail plate and hair shaft. The numbers of unique peptides, means, and standard deviations of four independent samples, obtained for the particulate fraction remaining after extensive detergent extraction are illustrated for (a) junctional and membrane proteins, (b) keratins and keratin associated proteins, and (c) the remaining cellular proteins. The 50 proteins with the highest number of unique peptides from hair and from nail samples are merged and illustrated in order of decreasing unique peptides for the nail samples.

analyses were conducted on (a) fingernail samples from four Caucasian volunteers, (b) four fingernail samples, and (c) four scalp hair samples provided by volunteers from Inner Mongolia, China. Each sample was extracted exhaustively with SDS under reducing conditions, producing a soluble fraction and an insoluble fraction comprising ≈90% and ≈10% of the total protein, respectively. For present purposes, a protein was considered identified when at least two unique peptides were detected in at least two of the samples in each group of four (listed in Supporting Information Table S1).

In the Caucasian fingernail samples, 144 proteins were identified. Of these, 97% were found in the detergent insoluble (cross-linked) fraction; of the 30 proteins identified in the

Table 2. Expression of Genes Encoding Select Prominent Constituents in Corneocyte Cross-Linked Proteome[a]

tissue/marker	DSP	JUP	PPL	AHNAK	ANXA1	SEBP1	EVPL	PKP1	FLG2	KPRP	LRRC15	VSIG8
Brain	33.62	30.37	32.14	30.60	28.50	29.83	ND	35.50	ND	ND	ND	ND
Placenta	24.73	23.71	27.31	21.14	19.71	28.28	26.83	28.25	ND	ND	29.50	35.88
Lung	29.87	25.72	28.77	22.18	21.39	25.77	26.86	29.86	ND	ND	38.60	35.28
Liver	27.03	24.58	27.63	22.69	24.64	22.89	34.62	ND	ND	ND	ND	38.84
Heart	24.84	24.63	31.00	22.65	24.88	27.32	ND	35.39	ND	ND	ND	ND
Skeletal Muscle	34.92	26.67	32.49	23.94	25.80	26.94	ND	33.29	ND	ND	ND	ND
Kidney	26.78	23.98	28.49	22.28	24.66	24.38	25.39	32.17	ND	ND	ND	33.27
Pancreas	23.60	23.77	26.15	21.34	23.88	25.00	24.87	32.16	ND	ND	ND	ND
Prostate	27.28	25.64	27.75	23.92	23.22	25.83	27.02	27.92	ND	ND	ND	ND
Testis	30.81	27.60	29.99	24.86	27.00	28.35	30.32	34.59	36.00	ND	ND	35.41
Ovary	28.76	25.62	28.47	21.04	23.69	25.22	31.14	34.40	ND	ND	ND	35.80
Small Intestine	31.04	27.30	29.22	22.67	24.43	25.77	27.97	33.59	ND	ND	ND	ND
Colon	27.96	26.91	29.47	23.41	25.27	23.75	28.25	35.50	ND	ND	ND	ND
Thymus	27.38	26.63	28.26	23.59	24.31	27.55	29.62	27.28	32.81	ND	ND	34.22
Spleen	28.83	27.02	34.02	22.76	24.37	25.47	37.34	ND	ND	ND	ND	38.06
Leukocyte	35.50	27.80	ND	21.87	22.49	33.50	34.91	ND	ND	ND	ND	38.35
Epidermis 1	19.96	20.30	23.06	21.96	24.94	28.73	26.37	21.88	20.99	23.92	33.89	ND
Epidermis 2	19.73	20.01	23.10	21.79	24.28	29.00	25.36	21.60	20.17	24.63	34.41	ND
Culture 1	17.96	18.08	18.93	19.62	17.36	29.93	22.96	19.89	19.99	17.75	34.97	ND
Culture 2	17.86	17.98	19.17	18.92	17.92	28.98	22.45	19.24	20.48	19.83	37.11	ND

[a] Ct values for β-actin were 21.4 $\pm$ 1.4 in the commercial panel, 23.5 $\pm$ 0.1 for the skin samples, and 19.8 $\pm$ 0.03 for the cultures. ND, not detected (Ct $\geq$ 40).

detergent solubilized fraction, 26 were also detected in the insoluble fraction. A subset of prominent proteins, those detected in all four samples, is listed in Table 1 (see Table S2 for details) in order of estimated relative abundance (emPAI). Also given are the numbers of unique peptides detected on which such calculations are empirically based.[23,26] The emPAI values are only semiquantitative, but they provide a convenient ranking of high-, medium-, and low-abundance proteins.[27] Among those listed in the solubilized fraction, 19 of the 21 are keratins and KAPs, accounting for 99% of the protein on a molar basis by this calculation. In contrast, although containing a large keratin component (≈60%), the insoluble fraction displayed a substantial fraction of cytoplasmic proteins (≈26%), membrane and junctional proteins (≈9%), and histones (≈5%).

Similar results were obtained with the fingernail samples provided by volunteers from Inner Mongolia. A total of 172 proteins were identified, with 50 found in the solubilized fraction. Of those identified in the latter, a large majority (86%) were also found in the insoluble (cross-linked) fraction, as in the Caucasian nail group. The proteins detected only in the solubilized fraction were of relatively low abundance judging by relatively low numbers of unique peptides. Most cytoskeletal proteins were readily detected in the solubilized and insoluble fractions, whereas membrane and other noncytoskeletal proteins were detected much better in the insoluble fraction (Figure 1). In the hair samples, analyzed in parallel, a total of 140 proteins were identified, 30 in the solubilized fraction, of which 24 were also seen in the insoluble fraction. The contrast in detection in the two fractions is illustrated in Figure 2.

The profile of proteins identified in nail plate and hair shaft exhibited numerous common constituents. To illustrate the degree of overlap, the 50 proteins with the highest number of unique peptides from the nail and hair samples from Mongolian volunteers were compared. As shown in Figure 3a, the combined profiles displayed similar peptide yields for nearly half the cytoskeletal proteins (keratins and KAPs) and appeared distinct for the rest. The most striking keratin differences were among those typical of epidermis (K5, K14, K17), whereas K82 was found only in hair. Among the 11 junctional and membrane proteins in the combined profiles, all were present in the nail samples, but two (EPPK1 and DSG1) were not detected in hair samples (Figure 3b). The remaining (intracellular) proteins overlapped considerably, but several appeared distinct. KPRP, SERPINB2, and CKB were detected only in nail, whereas CTTNB1 and ATP5B were seen only in hair (Figure 3c).

Examination of the membrane proteins observed in the cross-linked nail and hair samples revealed two prominent components about which little functional information is available, LRRC15 and VSIG8. To determine whether these are keratinocyte-specific, expression levels were measured in commercial preparations of cDNA from pools of a spectrum of 16 donor tissues (Table 2). As expected, the junctional proteins DSP, JUP, and PPL were widely expressed. So were AHNAK, ANXA1, and SEBP1, while EVPL and PKP1 were nearly as widely expressed. However, FLG2, KPRP, LRRC15, and VSIG8 were detected only at very low levels in some tissues and not at all in most. KPRP was found only in nail plate and epidermis, and FLG2 only in epidermis.

The samples obtained from Mongolia provided an opportunity to examine effects of systemic arsenic exposure on relative protein levels in hair shaft and nail plate. Comparison of the results from arsenic exposed and unexposed samples (Table S3) did not offer convincing evidence of major perturbation of the protein profiles. From the nail samples, two proteins from which fewer unique peptides were obtained in the samples from individuals exposed to high arsenic levels in drinking water (PKP1, DSG4) were examined further by multiple reaction monitoring. Monitoring transitions of one proteotypic peptide from each protein in the presence of the corresponding isotopically labeled control peptide did not give significantly altered yields ($p > 0.3$ and 0.08) in samples from individuals with high arsenic exposure (see Supplementary Figure 1). While not definitive, the data indicated such analysis would not provide a routine biomarker of effect.

Discussion

This is the first report identifying cross-linked proteins of nail plate. As found originally for human hair,[17] the profile of

solubilized proteins was much less complex than that of the nonsolubilizable proteins for both nail and hair. The latter fraction is composed of cytoskeletal, junctional, and a large variety of other intracellular proteins rendered insoluble by extensive isopeptide cross-linking.[28] Although low in relative amount (emPAI value of 0.14), the finding of TGM3 as a component of this fraction (Table S1) implicates it in cross-linking. The complexity of the protein profile obtained for the hair shaft, formed from three cell types of different morphology from divergent lineages in the hair follicle, can be attributed in part to its morphological complexity.[21] However, the complexity of the nail plate proteome was similar. This finding testifies to the propensity of corneocyte transglutaminases to incorporate many proteins in their immediate vicinity into cross-linked structures upon terminal cell maturation. A variation of the "dustbin hypothesis" proposed for the epidermis,[29] and noted in cultured epidermal cells as well,[30] this process makes efficient use of available resources to produce structures with great mechanical stability.

The present detailed comparison of prominent proteins is compatible with earlier analyses of keratin expression. The major keratins reported in the matrix were all identified (KRTs 1, 5, 10, 14, 17, 31, 34, 81, 85, 86), although several reported at very low levels (KRTs 7, 8, 18[10] and 38[11]) were not detected in our analysis. While their cellular localization was not studied at present, previous findings that both hair and epidermal keratins are present in nail plate is evident in the considerable overlap among the proteins identified in nail plate and hair shaft. Moreover, in addition to the hard keratins, DSG4 and SFN, most notable in the nail/hair overlap were SELENBP1, LRRC15, and VSIG8, all of uncertain function. PRDX6, present in nail (and hair) samples (Table 1), is found in all major organs[31] and is known to be cytoprotective in the epidermis.[32] Compatible with observations in the nail matrix,[11] hair keratin KRT85 was readily detected, but its usual partner, KRT35, was detected only at very low levels.

Until reported in hair,[17] LRRC15 was known normally to be expressed at low levels only in placenta, but it could be induced in neoplastic or certain other pathological conditions.[33,34] Using tissue cDNA from the mouse, KPRP was found to be expressed in the stomach (as well as skin), probably reflecting a contribution of stratified squamous epithelium in forestomach.[35] Found in the epidermis, notably in the granular layer,[36] expression of FLG2 in other stratified squamous epithelia is uncertain. These gene products provide novel corneocyte markers whose transcriptional regulation and function will be of interest to elucidate.

Considerable effort has been expended on finding biomarkers of arsenic exposure and effect in large populations of afflicted individuals in Taiwan,[37] Bangladesh,[38] and elsewhere. These are anticipated to help evaluate proposed mechanisms of action such as arsenic-induced oxidative stress[39] and to gauge interaction of arsenic exposure with exposure to metals such as cadmium.[40] Since only a fraction of exposed populations exhibit adverse effects, biomarkers could indicate sensitive individuals. Chronic arsenic exposure is commonly monitored using samples of nail plate,[16] so further analysis of such samples could reveal protein biomarkers of exposure and even help elucidate signaling pathways that are perturbed. Clear and reproducible alteration in levels of certain proteins in present work was not observed in either hair shaft or nail plate. Previous examination of hair ultrastructure in cross-section after extensive detergent extraction also did not detect perturbations induced by drinking water with high arsenic content.[41] Nevertheless, the possibility remains that such samples (or those of epidermis) from individuals showing adverse skin effects of arsenic exposure could display altered protein profiles. The possibility that such measurements could distinguish sensitive individuals in a population merits exploration.

Acknowledgment. We thank Drs. Young Jin Lee and Rich Eigenheer for expert technical assistance with mass spectrometry, Ms. Qin Qin for real-time PCR measurements and Dr. Judy L. Mumford for valuable discussion. This work was supported by USPHS grant P42 ES04699 from the National Institute of Environmental Health Sciences and a research grant from the Foundation for Ichthyosis and Related Skin Types.

Supporting Information Available: Figure S1, MRM data for peptides IQVVDVR and SPNQNVQQAAAGALR; Table S1, peptide data for identified proteins; Table S2, calculations of relative abundance using emPAI values; Table S3, comparisons of hair and nail proteomes as a function of arsenic exposure. This material is available free of charge via the Internet at http://pubs.acs.org.

References

(1) van de Kerkhof, P. C.; Pasch, M. C.; Scher, R. K.; Kerscher, M.; Gieler, U.; Haneke, E.; Fleckman, P. Brittle nail syndrome: a pathogenesis-based approach with a proposed grading system. *J. Am. Acad. Dermatol.* **2005**, *53*, 644–51.
(2) Tosti, A.; Iorizzo, M.; Piraccini, B. M.; Starace, M. The nail in systemic disease. *Dermatol. Clin.* **2006**, *24*, 341–7.
(3) Piraccini, B. M.; Iorizzo, M.; Starace, M.; Tosti, A. Drug-induced nail diseases. *Dermatol. Clin.* **2006**, *24*, 387–91.
(4) Norgett, E. E.; Wolf, F.; Balme, B.; Leigh, I. M.; Perrot, H.; Kelsell, D. P.; Haftek, M. Hereditary 'white nails': a genetic and structural study. *Br. J. Dermatol.* **2004**, *151*, 65–72.
(5) Daniel, C. R. I.; Piraccini, B. M.; Tosti, A. The nail and hair in forensic science. *J. Am. Acad. Dermatol.* **2004**, *50*, 258–61.
(6) Sprecher, E. Genetic hair and nail disorders. *Clin. Dermatol.* **2005**, *23*, 47–55.
(7) Lynch, M. H.; O'Guin, W. M.; Hardy, C.; Mak, L.; Sun, T. T. Acidic and basic hair/nail ("hard") keratins: their colocalization in upper cortical and cuticle cells of the human hair follicle and their relationship to "soft" keratins. *J. Cell Biol.* **1986**, *103*, 2593–606.
(8) Heid, H. W.; Moll, I.; Franke, W. W. Patterns of expression of trichocytic and epithelial cytokeratins in mammalian tissues. II. Concomitant and mutually exclusive synthesis of trichocytic and epithelial cytokeratins in diverse human and bovine tissues (hair follicle, nail bed and matrix, lingual papilla, thymic reticulum). *Differentiation* **1988**, *37*, 215–30.
(9) Kitahara, T.; Ogawa, H. Cellular features of differentiation in the nail. *Microsc. Res. Tech.* **1997**, *38*, 436–43.
(10) De Berker, D.; Wojnarowska, F.; Sviland, L.; Westgate, G. E.; Dawber, R. P.; Leigh, I. M. Keratin expression in the normal nail unit: markers of regional differentiation. *Br. J. Dermatol.* **2000**, *142*, 89–96.
(11) Perrin, C.; Langbein, L.; Schweizer, J. Expression of hair keratins in the adult nail unit: an immunohistochemical analysis of the onychogenesis in the proximal nail fold, matrix and nail bed. *Br. J. Dermatol.* **2004**, *151*, 362–71.
(12) Perrin, C. Expression of follicular sheath keratins in the normal nail with special reference to the morphological analysis of the distal nail unit. *Am. J. Dermopathol.* **2007**, *29*, 543–50.
(13) Jager, K.; Fischer, H.; Tschachler, E.; Eckhart, L. Terminal differentiation of nail matrix keratinocytes involves upregulation of DNase 1L2 but is independene of caspase-14 expression. *Differentiation* **2007**, *75*, 939–46.
(14) Rice, R. H.; Mehrpouyan, M.; Qin, Q.; Phillips, M. A. Transglutaminases in keratinocytes. In *The Keratinocyte Handbook*; Leigh, I. M., Lane, B., Watt, F. M., Eds.; Cambridge University Press: Cambridge, England, 1994; pp 259−74.
(15) Rice, R. H.; Crumrine, D.; Hohl, D.; Munro, C. S.; Elias, P. M. Cross-linked envelopes in nail plate in lamellar ichthyosis. *Br. J. Dermatol.* **2003**, *149*, 1050–4.

(16) Schmitt, M. T.; Schreinemachers, D.; Wu, K.; Ning, Z.; Zhao, B.; Le, X. C.; Mumford, J. L. Human nails as a biomarker of arsenic exposure from well water in Inner Mongolia: comparing atomic fluorescence spectrometry and neutron activation analysis. *Biomarkers* **2005**, *10*, 95–104.
(17) Lee, Y. J.; Rice, R. H.; Lee, Y. M. Proteome analysis of human hair shaft: From protein identification to posttranslational modification. *Mol. Cell. Proteomics* **2006**, *5*, 789–800.
(18) Rice, R. H.; Means, G. E.; Brown, W. D. Stabilization of bovine trypsin by reductive methylation. *Biochim. Biophys. Acta* **1977**, *492*, 316–21.
(19) Keller, A.; Nesvizhskii, A. I.; Kolker, E.; Aebersold, R. Empirical statistical model to estimate the accuracy of peptide identifications made by MS/MS and database search. *Anal. Chem.* **2002**, *74*, 5383–92.
(20) Nesvizhskii, A. I.; Keller, A.; Kolker, E.; Aebersold, R. A statistical model for identifying proteins by tandem mass spectrometry. *Anal. Chem.* **2003**, *75*, 4646–58.
(21) Rice, R. H.; Rocke, D. M.; Tsai, H.-S.; Lee, Y. J.; Silva, K. A.; Sundberg, J. P. Distinguishing mouse strains by proteomic analysis of pelage hair. *J. Invest. Dermatol.* **2009**, *129*, 2120–5.
(22) Shimomura, Y.; Wajid, M.; Zlotogorskic, A.; Lee, Y. J.; Rice, R. H.; Christiano, A. M. Founder mutations in the lipase H (LIPH) gene in families with autosomal recessive woolly hair/hypotrichosis. *J. Invest. Dermatol.* **2009**, *129*, 1927–34.
(23) Ishihama, Y.; Oda, Y.; Tabata, T.; Sato, T.; Nagasu, T.; Rappsilber, J.; Mann, M. Exponentially modified protein abundance index (emPAI) for estimation of absolute protein amount in proteomics by the number of sequenced peptides per protein. *Mol. Cell. Proteomics* **2005**, *4*, 1265–72.
(24) Macdiarmid, J.; Wilson, J. B. Separation of epidermal tissue from underlying dermis and primary keratinocyte culture. *Methods Mol. Biol.* **2001**, *174*, 401–10.
(25) Allen-Hoffmann, B. L.; Rheinwald, J. G. Polycyclic aromatic hydrocarbon mutagenesis of human epidermal keratinocytes in culture. *Proc. Natl. Acad. Sci. U.S.A.* **1984**, *81*, 7802–6.
(26) Ishihama, Y.; Schmidt, T.; Rappsilber, J.; Mann, M.; Hartl, F. U.; Kerner, M. J.; Frishman, D. Protein abundance profiling of the Escherichia coli cytosol. *BMC Genomics* **2008**, *9*, 102.
(27) Seibert, C.; Davidson, B. R.; Fuller, B.; Patterson, L. H.; Griffiths, W. J.; Wang, Y. Multiple approaches to the identification and quantification of cytochromes P450 in human liver tissue by mass spectrometry. *J. Proteome Res.* **2009**, *8*, 1672–81.
(28) Rice, R. H.; Wong, V. J.; Pinkerton, K. E. Ultrastructural visualization of cross-linked protein features in epidermal appendages. *J. Cell Sci.* **1994**, *107*, 1985–92.
(29) Michel, S.; Schmidt, R.; Robinson, S. M.; Shroot, B.; Reichert, U. Identification and subcellular distribution of cornified envelope precursor proteins in the transformed human keratinocyte line SV-K14. *J. Invest. Dermatol.* **1987**, *88*, 301–5.
(30) Robinson, N. A.; Lapic, S.; Welter, J. F.; Eckert, R. L. S100A11, S100A10, annexin I, desmosomal proteins, small proline-rich proteins, plasminogen activator inhibitor-2, and involucrin are components of the cornified envelope of cultured human epidermal keratinocytes. *J. Biol. Chem.* **1997**, *272*, 12035–46.
(31) Manevich, Y.; Fisher, A. B. Peroxiredoxin 6, a 1-Cys peroxiredoxin, functions in antioxidant defense and lung phospholipid metabolism. *Free Radical Biol. Med.* **2005**, *38*, 1422–32.
(32) Kumin, A.; Huber, C.; Rulicke, T.; Wolf, E.; Werner, S. Peroxiredoxin 6 is a potent cytoprotective enzyme in the epidermis. *Am. J. Pathol.* **2006**, *169*, 1194–205.
(33) Reynolds, P. A.; Smolen, G. A.; Palmer, R. E.; Sgroi, D.; Yajnik, V.; Gerald, W. L.; Haber, D. A. Identification of a DNA-binding site and transcriptional target for the EWS-WT1(+KTS) oncoprotein. *Genes Dev.* **2003**, *17*, 2094–107.
(34) Satoh, K.; Hata, M.; Shimizu, T.; Yokota, H.; Akatsu, H.; Yamamoto, T.; Kosaka, K.; Yamada, T. Lib, transcriptionally induced in senile plaque-associated astrocytes, promotes glial migration through extracellular matrix. *Biochem. Biophys. Res. Commun.* **2005**, *23*, 631–6.
(35) Lee, W. H.; Jang, S.; Lee, J. S.; Lee, Y.; Seo, E. Y.; You, K. H.; Lee, S. C.; Nam, K. I.; Kim, J. M.; Kee, S. H.; Yang, J. M.; Seo, Y. J.; Park, J. K.; Kim, C. D.; Lee, J. H. Molecular cloning and expression of human keratinocyte proline-rich protein (hKPRP), an epidermal marker isolated from calcium-induced differentiating keratinocytes. *J. Invest. Dermatol.* **2005**, *125*, 995–1000.
(36) Toulza, E.; Mattiuzzo, N. R.; Galliano, M. F.; Jonca, N.; Dossat, C.; Jacob, D.; de Daruvar, A.; Wincker, P.; Serre, G.; Guerrin, M. Large-scale identification of human genes implicated in epidermal barrier function. *Genome Biol.* **2007**, *8*, R107.
(37) Chen, C. J.; Hsu, L. I.; Wang, C. H.; Shih, W. L.; Hsu, Y. H.; Tseng, M. P.; Lin, Y. C.; Chou, W. L.; Chen, C. Y.; Lee, C. Y.; Wang, L. H.; Cheng, Y. C.; Chen, C. L.; Chen, S. Y.; Wang, Y. H.; Hsueh, Y. M.; Chiou, H. Y.; Wu, M. M. Biomarkers of exposure, effect, and susceptibility of arsenic-induced health hazards in Taiwan. *Toxicol. Appl. Pharmacol.* **2005**, *206*, 198–206.
(38) Chen, Y.; Parvez, F.; Gamble, M.; Islam, T.; Ahmed, A.; Argos, M.; Graziano, J. H.; Ahsan, H. Arsenic exposure at low-to-moderate levels and skin lesions, arsenic metabolism, neurological functions, and biomarkers for respiratory and cardiovascular diseases: review of recent findings from the Health Effects of Arsenic Longitudinal Study (HEALS) in Bangladesh. *Toxicol. Appl. Pharmacol.* **2009**, *239*, 184–92.
(39) De Vizcaya-Ruiz, A.; Barbier, O.; Ruiz-Ramos, R.; Cebrian, M. E. Biomarkers of oxidative stress and damage in human populations exposed to arsenic. *Mutat. Res.* **2009**, *674*, 85–92.
(40) Nordberg, G. F. Biomarkers of exposure, effects and susceptibility in humans and their application in studies of interactions among metals in China. *Toxicol. Lett.* **2009**, *192*, 45–9.
(41) Rice, R. H.; Crumrine, D.; Uchida, Y.; Gruber, R.; Elias, P. M. Structural changes in epidermal scale and appendages as indicators of defective TGM1 activity. *Arch. Dermatol. Res.* **2005**, *297*, 127–33.

PR1009349